Electronic Supplementary Information (ESI)

Novel left-handed double-helical chiral carbon nanotube for electrochemical biosensing study

Shuang Ren,[a] Huan Wang,[a]* Yufan Zhang,[a] Liping Guo,[b] Hongyi Zhang,[a]* Zhihong Shi,[a] Yuena Sun,[a] Mingjie Li,[a] Meng Li,[a] Zheng Huang[a]

a Key Laboratory of Analytical Science and Technology of Hebei Province, College of Chemistry and Environmental Science, Hebei University, Baoding 071002, Hebei Province, P. R. China.

b Faculty of Chemistry, Northeast Normal University, Changchun, 130024, P. R. China

*Corresponding Author:

Huan Wang**,** College of Chemistry and Environmental Science, Hebei University, Baoding 071002, Hebei Province, P. R. China**,** Email:zwhsjzl@163.com;
Hongyi Zhang, College of Chemistry and Environmental Science, Hebei University, Baoding 071002, Hebei Province, P. R. China**,** Email:freetime20100401@163.com.

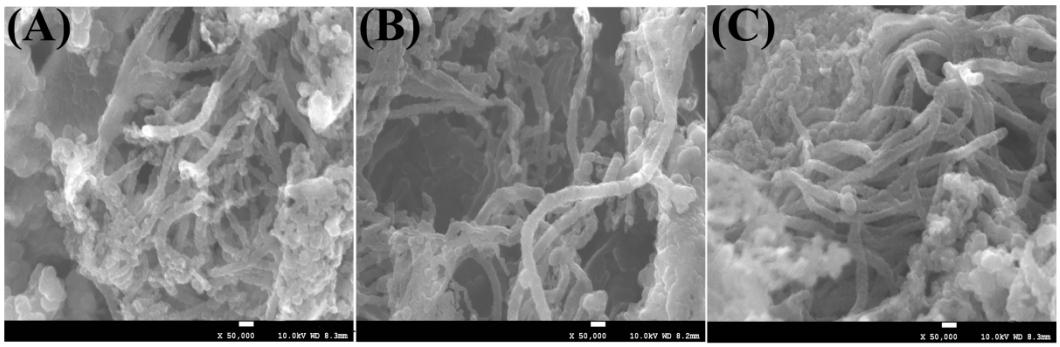

Fig. S1: SEM images of CCNT-500 (A), CCNT-700 (B) and CCNT-900 (C) at low resolution.

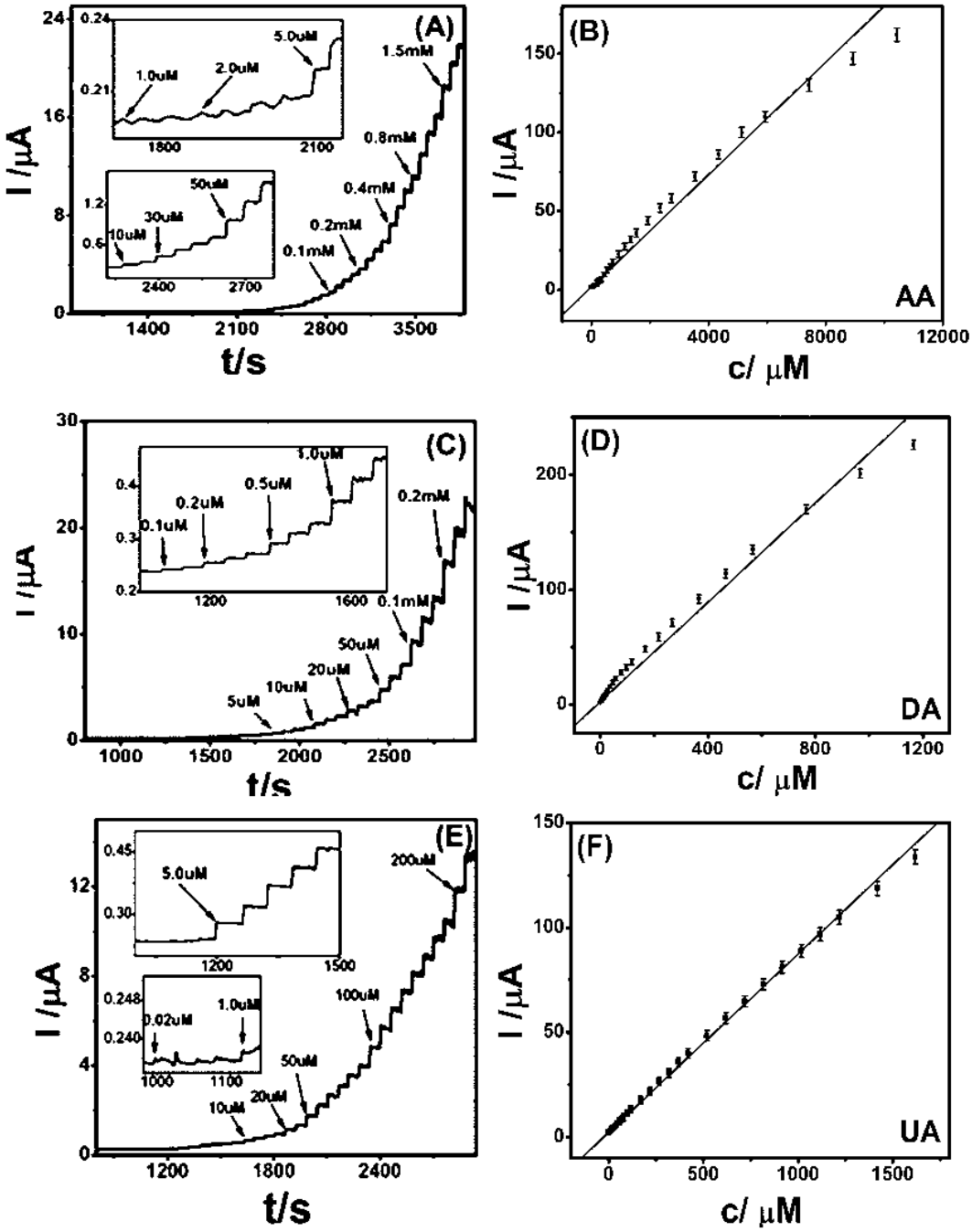

Fig. S2: (A) Current-time curves for the CCNT-900/GCE with successive additions different concentration (μM) of AA in 0.1 M PBS (pH 7.4). Operating potential: 0.00 V. (B) The linear relationship between AA concentration and current signal. (C) Current-time curves for the CCNT-900/GCE with successive additions different concentration (μM) of DA in a 0.1 M PBS (pH 7.4). Operating potential: 0.20 V. Inset is the amperometric response with successive addition of DA at lower concentration. (D) The linear relationship between DA concentration and current signal. (E) Current-time curves for the CCNT-900/GCE with successive additions different concentration (μM) of UA in a 0.1 M PBS (pH 7.4). Operating potential: 0.30 V. (F) The linear elationship between UA concentration and current signal.

Table S1: Structure properties of the as-synthesized CCNT-x at different carbonization temperature

Samples (carbonization temperature)	Surface area[a] m^2g^{-1}	Pore size[b] nm	N-bonding configurations
CCNT-500 (500℃)	77.51	20.8	pyridinic N 4.24% pyrrolic N 1.40% graphitic N 0.24%
CCNT-700 (700℃)	190.88	20.8	pyridinic N 2.79% pyrrolic N 1.30% graphitic N 0.38%
CCNT-900 (900℃)	242.64	22.8	pyridinic N 0.72% pyrrolic N 0.53% graphitic N 0.48%

[a] Surface area was obtained based on the Brunauer-Emmett-Teller (BET) method. [b] The pore size was obtained based on the BJH method

Table S2: Characteristics of simultaneous determination of AA, DA and UA on CCNT-900/GCE in 0.1 M PBS solution (pH 7.4)

Solution	Additions	Linear range (μM)	Linear equation (μA, μM)	Regression	Limit of detection (S/N=3)	RSD (LOQ)
5 μM DA 10 μM UA 80 μM AA 20 μM UA 50 μM AA 3 μM DA	AA	10-1280	I=11.35+0.018c	0.9972	1.33	1.7%
	DA	1-124	I=8.78+0.206c	0.9915	0.13	1.1%
	UA	10-500	I=5.65+0.032c	0.9948	0.75	1.6%

Table S3: Electrocatalytic performance comparison of different modified electrodes towards H_2O_2 detection

modified electrodes	Linear range (μM)	Detection limit (μM)	Reference
Hb/SA–MWCNTs/GCE	40-200	16.4	[1]
ZnO/Au/Nafion/HRP/GCE	15-1100	9.0	[2]
Cu_2O/graphene	300-7800	20.8	[3]
PMo_{12}-PPy	200-3000	50	[4]
PDDA-rGO/AgNPs	100-4100	35	[5]

CCNT-900/GCE	20-60000	2.0	This work

Table S4: Electrocatalytic performance comparison of different modified electrodes towards NADH detection

modified electrodes	Limit of detection (μM)	Linear range (μM)	Sensitivity (μA μM^{-1})	Refenrence
graphene/GCE	20.00	50-1400	0.0126	[6]
PGE	15	0.5-100	0.000975	[7]
CR-GO/GCE	10.00	40-800	0.000189	[8]
APTS-Fe_3O_4/PDC/GCE	0.01	0.05-25	0.5545	[9]
Au-TiO_2/GR/GCE	0.20	10-240	0.0162	[10]
CCNT-900/GCE	0.035	0.1-400	0.0822	This work

Reference

1 H.Y. Zhao, W. Zheng, Z.X. Meng, H.M. Zhou, X.X. Xua, Z. Li and Y.F. Zheng, Bioelectrochemistry of hemoglobin immobilized on a sodium alginate-multiwall carbon nanotubes composite film. *Biosens Bioelectron*, 2009, **24**, 2352.

2 C.L. Xiang, Y.J. Zou, L.X. Sun and F. Xu, Direct electrochemistry and enhanced electrocatalysis of horseradish peroxidase based on flowerlike ZnO-gold nanoparticle-nafion nanocomposite. *Sens Actuators B*, 2009, **136**, 158.

3 M. Liu, R. Liu and W. Chen, Graphene wrapped Cu_2O nanocubes: Non-enzymatic electrochemical sensors for the detection of glucose and hydrogen peroxide with enhanced stability. *Biosens Bioelectron*, 2013, **45**, 206.

4 X. Wang, H. Zhang, E. Wang, Z. Han and C. Hu, Phosphomolybdate-polypyrrole composite bulk-modified carbon paste electrode for a hydrogen peroxide amperometric sensor. *Mater Lett*, 2004, **58**, 1661.

5 X. Liu, X. Xu, H. Zhu and X. Yang, Synthesis of graphene nanosheets with incorporated silver nanoparticles for enzymeless hydrogen peroxide detection. *Anal Meth*, 2013, **5**, 2298.

6 K. Guo, K. Qian, S. Zhang, J.L. Kong, C.Z. Yu and B.H. Liu, Bio-electrocatalysis of NADH and ethanol based on graphene sheets modified electrodes. *Talanta*, 2011, **85**, 1174.

7 N.S. Lawrence and J. Wang, Chemical adsorption of phenothiazine dyes onto carbon nanotubes: toward the low potential detection of NADH. *Electrochem Commun*, 2006, **8**, 71.

8 M. Zhou, Y. Zhai and S. Dong, Electrochemical Sensing and biosensing platform based on

chemically reduced graphene oxide. *Anal Chem*, 2009, **81**, 5603.

9 L. Cui, S. Ai, K. Shang, X. Meng and C. Wang, Electrochemical determination of NADH using a glassy carbon electrode modified with Fe_3O_4 nanoparticles and poly-2,6-pyridinedicarboxylic acid, and its application to the determination of antioxidant capacity. *Microchim Acta*, 2011, **174**, 31.

10 Y. Fan, X. Yang, C. Yang and J. Liu, Au-TiO_2/graphene nanocomposite film for electrochemical sensing of hydrogen peroxide and NADH. *Electroanalysis*, 2012, **24**, 1334.